efficient indirect superexchange pathway than does urea. The fact that relatively strong exchange interactions may be transmitted through two halide ions is not without precedent. Indirect pathways of the type [M-X···X-M] have been shown to produce fairly strong exchange ($J \sim 5$-10 cm^{-1}) in the Ir(IV)-Ir(IV) pairs observed in iridium-doped crystals of K_2PtCl_6 and $(NH_4)_2PtCl_6$.[25,26] In this case the dimer is formed from two octahedral [$IrCl_6^{2-}$] complexes which interact along a common twofold axis. It is unfortunate that a more quantitative discussion of the magnetic interactions in Cr(III)-Cr(III) pairs is prevented by the lack of accurately determined exchange energies.

Conclusions

It is clear that the Cr(III) impurities in the doped $CsMX_3$ crystals are incorporated into the lattice in a highly selective manner. The selectivity appears to arise from the rather strict charge compensation requirement of the host lattices. The charge compensation requirement is primarily an electrostatic effect and is not greatly dependent on the chemical properties of the impurity ions. It is reasonable to conclude that within rather broad limits any trivalent ion will behave like Cr(III) when doped into crystals which adopt the linear chain RMX_3 structure. From a spectroscopic point of view these systems are unique in that magnetically coupled pairs are produced in high relative concentrations, even at low doping levels. The fact that the distribution of a given trivalent ion can be manipulated by the introduction of other impurity ions makes it possible to control the nature of the spectroscopic species present in the doped crystals.

Acknowledgment. The authors wish to thank Professor B. B. Garrett of Florida State University for the use of the E-12 spectrometer and for helpful advice in obtaining the spectra.

References and Notes

(1) G. L. McPherson, L. J. Sindel, H. F. Quarls, C. B. Frederick, and C. J. Doumit, *Inorg. Chem.*, **14**, 1831 (1975).
(2) G. L. McPherson, T. J. Kistenmacher, and G. D. Stucky, *J. Chem. Phys.*, **52**, 815 (1970).
(3) G. L. McPherson, A. M. McPherson, and J. L. Atwood, to be published.
(4) G. L. McPherson and K. O. Devaney, *Inorg. Chem.*, **16**, 1565 (1977).
(5) H. Rinneberg and H. Hartmann, *J. Chem. Phys.*, **52**, 5814 (1970).
(6) G. L. McPherson, R. C. Koch, and G. D. Stucky, *J. Chem. Phys.*, **60**, 1424 (1974).
(7) G. L. McPherson and W. Heung, *Solid State Commun.*, **19**, 53 (1976).
(8) J. Owen, *J. Appl. Phys.*, **32**, 213S (1961).
(9) J. Owen and E. A. Harris, "Electron Paramagnetic Resonance", S. Geschwind, Ed., Plenum Press, New York, N.Y., 1972, pp 427-492.
(10) A. Abragam and B. Bleaney, "Electron Paramagnetic Resonance of Transition Metal Ions", Clarendon Press, Oxford, 1970.
(11) A. J. B. Codling and B. Henderson, *J. Phys. C*, **4**, 1409 (1971).
(12) S. R. P. Smith and J. Owen, *J. Phys. C*, **4**, 1399 (1971).
(13) M. J. Berggren, G. F. Imbusch, and P. L. Scott, *Phys. Rev.*, **188**, 675 (1969), and references cited therein.
(14) J. C. M. Henning, J. H. DenBoef, and G. G. P. van Gorkom, *Phys. Rev. B*, **7**, 1825 (1973).
(15) J. R. Beswick and D. E. Dugdale, *J. Phys. C*, **6**, 3326 (1973).
(16) P. C. Benson and D. E. Dugdale, *J. Phys. C*, **8**, 3872 (1975).
(17) E. A. Harris, *J. Phys. C*, **5**, 338 (1972).
(18) J. E. Wertz and P. Auzins, *Phys. Rev.*, **106**, 484 (1957).
(19) J. E. Wertz and P. Auzins, *J. Phys. Chem. Solids*, **28**, 1557 (1967).
(20) J. L. Patel, J. J. Davies, B. C. Cavenett, H. Takeuchi, and K. Horai, *J. Phys. C*, **9**, 129 (1976).
(21) G. L. McPherson and L. M. Henling, *Phys. Rev. B*, **16**, 1889 (1977).
(22) B. R. McGarvey, *J. Chem. Phys.*, **41**, 3743 (1964).
(23) B. B. Garrett, K. DeArmond, and H. S. Gutowsky, *J. Chem. Phys.*, **44**, 3393 (1966).
(24) P. H. Davis and R. L. Belford, *ACS Symp. Ser.*, **5**, 51 (1974).
(25) J. H. E. Griffiths, J. Owen, J. G. Park, and M. F. Partridge, *Proc. R. Soc. London, Ser. A*, **250**, 84 (1959).
(26) E. A. Harris and J. Owen, *Proc. R. Soc. London, Ser. A*, **289**, 122 (1965).

Electronic Selection Rules in the Photochemical Substitution Reactions of Cr(III) Complexes

L. G. Vanquickenborne* and A. Ceulemans

Contribution from the Department of Chemistry, University of Leuven, Celestijnenlaan 200F, B 3030 Heverlee, Belgium. *Received March 21, 1977*

Abstract: The stereochemistry of photoinduced substitution reactions of Cr(III) complexes has been analyzed by using orbital and state correlation diagrams. The experimentally observed stereomobility was considered to be the result of several steps: initiated by the selective loss of a ligand, the complex fragment undergoes an isomerization, followed by the nucleophilic attack of an entering ligand. Both isomerization and association reactions are shown to occur in a stereospecific way, controlled by the electronic structure of the complex. The analysis was carried out by means of a general computer program, incorporating both the effects of the ligand field potentials and of the interelectronic repulsion. The conclusions of this study point to the existence of electronic selection rules in the photochemical reaction pathways of transition metal complexes. These rules can be restated either in terms of the frontier orbital concept or in terms of the conservation of orbital symmetry.

Introduction

The experimental data on the photochemistry of Cr(III) complexes have been accumulating increasingly fast over the last years.[1,2] The first effort to systematize the photosubstitution behavior has led to Adamson's empirical rules.[3] These rules suggest that the relative spectrochemical strength of the different ligands is the main factor determining which ligand is exchanged.

From a more theoretical point of view, a number of authors[4,5] have attempted to explain, or at least to rationalize, Adamson's rules. Recently, we have developed a model that allows the prediction of the leaving ligand while using only simple ligand field considerations;[6] at the same time, the model provides an alternative to the original rules.

During the last few years, it became clear that the oriented labilization represents only *one* facet of the Cr(III) photochemistry. Another feature, almost equally clear cut, shows up in the stereochemical aspects of the substitution reactions. Kirk summarized the photostereochemistry as follows: "the entering ligand will stereospecifically occupy a position corresponding to entry into the coordination sphere trans to the leaving ligand".[7]

0002-7863/78/1500-0475$01.00/0

This behavior is even more remarkable when compared with the thermal substitution reactions of the same Cr(III) complexes, which are generally stereorigid. Here, the entering ligand apparently enters the coordination sphere cis to the leaving ligand.[2]

It is the purpose of this paper to relate the photostereochemical behavior of the Cr(III) complexes to their electronic wave functions and energies. Basically, the same principles will be applied as in our previous work on the prediction of the leaving ligand.[6] The conclusions can be aptly summarized by means of simple correlation diagrams and selection rules.

The Experimental Data. Most experimental data refer to the case of axial labilization, more specifically to *trans*-diacidotetramines, where the leaving ligand is situated on the heteroaxis, or to monoacidopentamines, where the leaving ligand is the axial NH_3.

In the case of diacidotetramines of the type *trans*-$Cr(NH_3)_4XY$ or *trans*-$Cr(en)_2XY$, the aquation product has a cis configuration to almost 100%:

$$trans\text{-}CrN_4XY + H_2O \xrightarrow{h\nu} cis\text{-}CrN_4X(H_2O) + Y$$

where Y is considered to be the leaving ligand. The stereomobility has been verified[8-11] for *trans*-$Cr(en)_2Cl_2^+$, -$Cr(en)_2(NCS)_2^+$, -$Cr(en)_2(NCS)Cl^+$, -$Cr(NH_3)_4(H_2O)Cl^{2+}$, and -$Cr(NH_3)_4(H_2O)NCS^{2+}$.

The analysis of the monoacidopentamines is more involved in that even the unequivocal identification of the end product as cis does not necessarily imply stereomobility. Indeed, since the leaving ligand is NH_3, it remained to be shown that this ligand is released from the heteroaxis, trans to X. The problem was solved in two different ways. By isotope labeling, Adamson and co-workers[12] were able to synthesize $Cr(NH_3)_4(^{15}NH_3)Cl^+$; from a statistical analysis of the photolysis products, they were able to deduce the trans position of the leaving NH_3 ligand. Wong and Kirk,[13] on the other hand, proved the axial labilization by the photolytic aquation of *trans*-$Cr(en)_2(NH_3)Cl^{2+}$. As a consequence of these results, the stereomobility of the photochemical pentamine aquations can be considered to be quite firmly established. The identification of the aquation product as a cis complex has been reported[2,14] for $Cr(NH_3)_5Cl^{2+}$, $Cr(NH_3)_5Br^{2+}$, $Cr(NH_3)_5(NCS)^{2+}$, $Cr(NH_3)_5(H_2O)^{3+}$, and $Cr(NH_3)_5(CF_3COO)^{2+}$.

There are two apparent exceptions to the rule of total stereomobility: (1) the product of the photochemical aquation of *trans*-$Cr(en)_2FCl^+$ (leaving ligand: Cl^-) is reported[15] to be indeed predominantly cis, but also about 10% trans product is formed; (2) the product of the photolytical aquation of $[Cr(cyclam)Cl_2]^+$ (leaving ligand: Cl^-) is trans.[16] As a matter of fact, one hardly expects the tetradentate cyclam ligand[17] to give rise to any kind of stereomobility. This might be the reason why the complex is almost totally photoinert (quantum yield $\sim 3 \times 10^{-4}$).

A few experimental data are reported on complexes, where the leaving ligand is not situated on the heteroaxis, but in the equatorial plane, perpendicular to this axis. This "equatorial labilization" appears to have its own stereochemical rules, characterized by the preservation of the heteroaxis.[9] Although the here proposed formalism might readily be extended to this case, the set of structural data is too limited to allow for generalizations at this point. In what follows, attention will be restricted exclusively to axially labilized complexes.

Mechanistic Considerations. Basically two different mechanisms were discussed at several occasions both by Adamson[18] and by Kirk.[7,13] First of all, substitution of *trans*-CrN_4XY can be thought of as initiated by the dissociation of the Y ligand, concerted with the rearrangement of the remaining complex from a tetragonal pyramid (TP) to a trigonal bipyramid (TBP). In this pentacoordinated intermediate, the X ligand can be either in apical or in equatorial position. The subsequent association with a solvent ligand should most probably proceed by lateral attack on one of the three sides of the equatorial triangle. If X is in apical position, such an association leads exclusively to a cis product; if X is in equatorial position, simple statistics would predict $^2/_3$ cis and $^1/_3$ trans product.

Alternatively, one might think of the substitution reaction as proceeding via a seven-coordinated state, formed from the association of the original—distorted—complex and a solvent molecule, with the consequent expulsion of the Y ligand.

It has been argued in the literature[2] that a backside attack on the complex would explain the stereomobility. This may be true, but it leaves unanswered the question why a backside attack would be the preferred reaction path. As a matter of fact, backside attack tends to give rise to a cis product, but frontside attack tends to give rise to a trans product.

Neither in five nor in seven coordination are simple statistics able to reproduce the experimental results. Apparently, some additional effect must be operative so as to ensure the almost exclusive production of the cis product.

The cyclam experiment, referred to in the previous section, cannot be considered to be a decisive indication.[18] Indeed, the observed photoinertness of the cyclam complex can be explained equally well by an associative process (the formation of the seven-coordinated complex of the appropriate structure will be hindered) as by a dissociative process (the five-coordinated intermediate will be unable to undergo the isomerization, necessary to assist in the concerted release of the departing ligand).

In what follows, we will adopt the hypothesis of a five-coordinated intermediate. Indeed, since the electronic excitation is the direct cause of the labilization of the Cr–Y bond, it seems inherently plausible that the dissociative step should be the initiator of the reaction. The fact that the leaving ligand has been shown[6] to be the one with the smallest bond strength in the original *undistorted* complex lends additional strength to this hypothesis.

An a posteriori argument against the seven-coordinated intermediate is that, even after close examination, no mechanism appears to be available to account for the exclusive formation of the cis product. The five-coordinated intermediate, on the other hand, does offer the possibility of rationalizing the observed stereochemistry, as we intend to show in what follows.

The photosubstitution reaction will thus formally be dissected into three separate processes: the dissociation of Y from the excited complex, the isomerization of the pentacoordinated intermediate, and the association of the isomerized intermediate with the entering ligand. It is obvious that these three processes will actually proceed in a more or less concerted way, and not simply consecutively. The factors determining the dissociative process have been treated in a previous paper[6] and will not further be considered here; the attention will be focused entirely on the latter two processes.

Method of Analysis. The zero-order ligand field wave functions can be written as linear combinations of Slater determinants, constructed from the usual real metal d orbitals.

The perturbation Hamiltonian is given by

$$\mathcal{H} = \sum_i \mathcal{V}_i + \sum_{i>j} \frac{e^2}{r_{ij}}$$

The first term in $\mathcal{H}$, written as a sum of one-electron operators, represents the ligand field potential. The second operator corresponds to the interelectronic repulsion enengy; i and j are electron labels. Spin–orbit coupling will be neglected throughout. The potential $\mathcal{V}_i$ is written as a sum of pertur-

Table I. Orbital Energy Expressions for the Different Five-Coordinate Fragments as a Function of the Individual (σ_L, π_L) Parameters

	Irreducible representation	Orbital energy
TP (C_{4v})	b_2	$E(xy) = 4\pi_N$
	e	$E(xz) = E(yz) = \pi_X + 2\pi_N$
	a_1	$E(z^2) = \sigma_X + \sigma_N$
	b_1	$E(x^2 - y^2) = 3\sigma_N$
TBP (C_{3v})	a_1	$E(z^2) = \sigma_X + {}^7/_4\sigma_N$
	e	$E(xy) = E(x^2 - y^2) = {}^9/_8\sigma_N + {}^3/_2\pi_N$
	e	$E(xz) = E(yz) = \pi_X + {}^5/_2\pi_N$
TBP (C_{2v})	a_2	$E(xy) = {}^7/_2\pi_N$
	b_1	$E(xz) = \pi_X + {}^5/_2\pi_N$
	b_2	$E(yz) = \pi_X + {}^9/_8\sigma_N + {}^1/_2\pi_N$
	a_1	$\mathcal{V}$ z^2 $x^2 - y^2$
		z^2 $\sigma_X + \frac{17}{32}\sigma_N$ $-\frac{(3)^{1/2}}{8}\left(\frac{13}{4}\sigma_N + \frac{9}{8}\pi_N - 3\pi_N\right)$
		$x^2 - y^2$ $-\frac{(3)^{1/2}}{8}\left(\frac{13}{4}\sigma_N - \frac{75}{32}\sigma_N + \frac{3}{8}\pi_N - 3\pi_N\right)$

bations, due to the individual ligands L:

$$\mathcal{V}_i = \sum_L \mathcal{V}_i^L$$

The matrix of $\mathcal{V}_i^L$ in the usual real d-orbital set is very simple[19,20] and diagonal when L is situated on the z axis:

$$\langle z^2|\mathcal{V}_i^{L_z}|z^2\rangle = \sigma$$

$$\langle xz|\mathcal{V}_i^{L_z}|xz\rangle = \langle yz|\mathcal{V}_i^{L_z}|yz\rangle = \pi$$

The diagonal elements of d_{xy} and $d_{x^2-y^2}$ are assumed to be zero when δ interactions are neglected. If the ligand L is situated on any other arbitrary axis p, specified by the polar coordinates (θ, ϕ), the matrix of $\mathcal{V}_i^{L_p}$ is no longer diagonal, but it can be calculated in a quite straightforward way; the 25 matrix elements are simple functions of σ, π, θ, and ϕ.[20] The name "angular overlap model" (AOM) which we and others have used previously to label this model[20-22] is, in fact, not entirely adequate. The parameters σ and π are semiempirical and are not necessarily related to overlap integrals. They do have a simple chemical interpretation in that they incorporate very neatly the energetic effect of the isolated metal–ligand interactions. The model describes in a very direct way the role of the angular position (θ_L, ϕ_L) of the individual ligands on the energy matrix. The radial position comes in only indirectly, through the value of the σ and π parameters. Therefore, the present version of the model might be more adequately classified as an additive point ligand model.

After diagonalization of the ligand field matrix, Slater determinants of the appropriate symmetry can be combined into eigenfunctions of $\mathcal{S}^2$; the matrix elements of the repulsion operator can be evaluated in terms of Racah B and C parameters.[23,24] A general computer program was developed to construct the relevant functions for an arbitrary d^n system, to set up the total energy matrix and to carry out its exact diagonalization. In this way, one avoids the shortcomings of both the weak field and the strong field approximations.

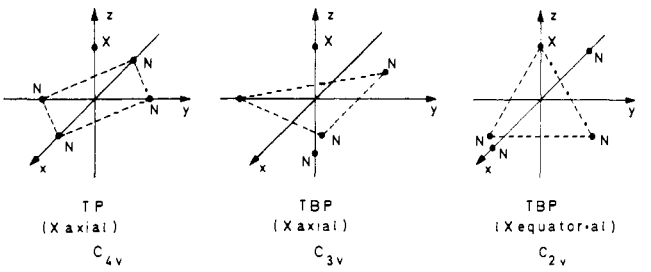

Figure 1. The tetragonal pyramid and the two trigonal bipyramids: geometry and coordinate systems used in the calculations.

Table II. Ligand Field Parameter Set for the Cr(III) Complexes (μm^{-1})

Racah Parameters for Cr^{3+} (d^3 system)
$B = 0.07$
$C = 0.30$

Cr(III)-L Interaction Parameters

Ligand	σ	π	Ref
NH_3	0.718	0.00	29
F	0.763	0.170	29, 30
H_2O	0.594	0.050	30
X	0.570	0.100	Average π donor

Along a given reaction path, the ligand field part of the perturbation Hamiltonian $\mathcal{V} = \sum_i \sum_L \mathcal{V}_i^L$ will vary, according to a certain specified set of ligand movements. For the isomerization reaction from the tetragonal pyramid to the trigonal bipyramid, the ligands are assumed to move on a sphere. Therefore, the individual σ and π parameters are taken to be constant, and the ligand movements consist of angular displacements only. For the association reaction, the parameters of the sixth ligand are varied from 0 to the σ, π values at equilibrium distance. In this way, orbital and state energy diagrams can be set up, showing the evolution of the system throughout the reaction.

Actually, correlation diagrams of this general type were first introduced by Woodward and Hoffmann in the theory of concerted organic reactions.[25] In organic chemistry one is usually led to the same set of conclusions, whether one uses orbital energy diagrams (original Woodward-Hoffmann procedure) or state energy diagrams (Longuet-Higgins and Abrahamson[26]). Because of the very pronounced effects of electron repulsion in the open shell d^n systems, one a priori expects that the treatment of transition metal reactions should certainly be carried out at the state level.[27] Later on, it will be shown, however, that it still remains possible—at least in the present case—to describe qualitatively the general features of the reactions in terms of simple orbital considerations.

The Isomerization Reaction. The starting point is the five-coordinated fragment resulting from the removal of Y in *trans*-CrN_4XY; if Y is removed without further change, one obtains a tetragonal pyramid with X in axial position and C_{4v} symmetry. As possible results from the isomerization reaction, one has to consider two trigonal bipyramids, one with X in apical position, the other one with X in equatorial position.[28]

(1) Orbital Correlation Diagrams. While the TBP skeleton has D_{3h} symmetry, the two bipyramids have C_{3v} and C_{2v} symmetry, respectively (Figure 1). Table I gives the energy expressions for the real d-orbital basis set. In order to obtain the numerical values of the energies, the parameter set of Table II was used throughout.

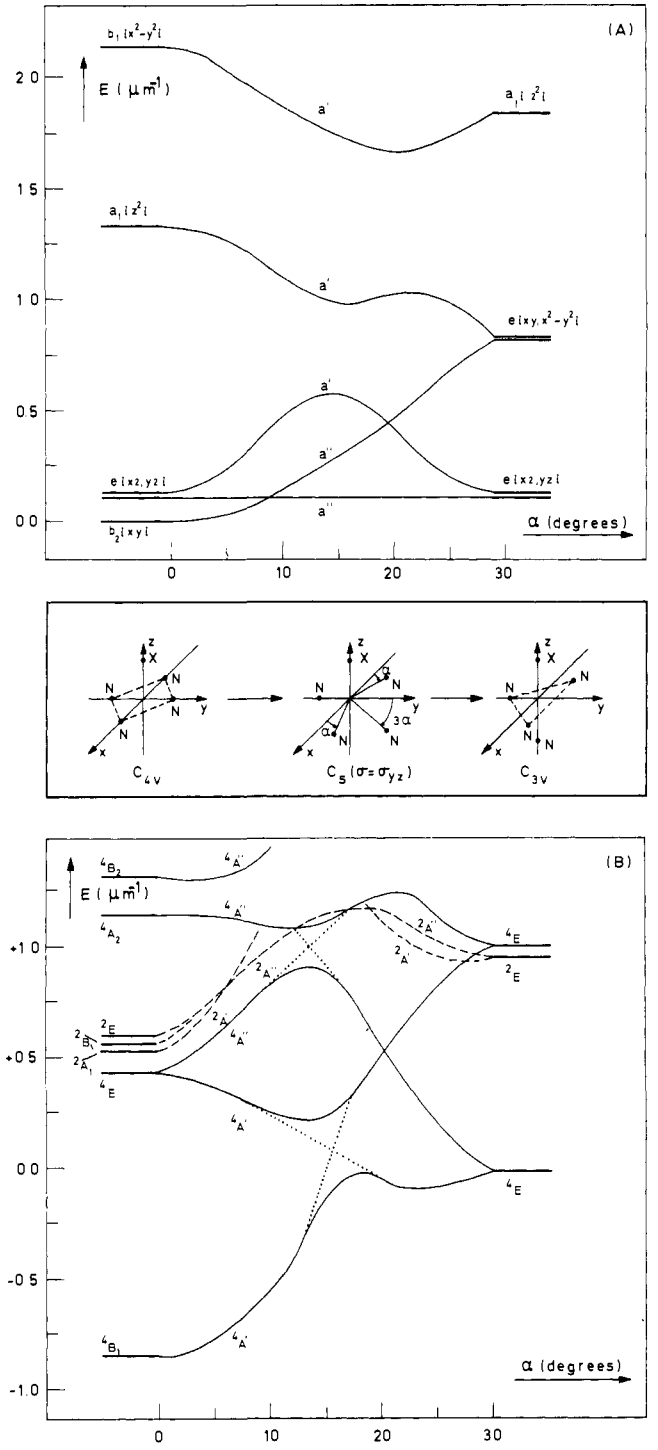

Figure 2. Orbital (A) and state (B) energy correlation diagram for the isomerization of a Cr^{3+} system from the tetragonal pyramid to the trigonal bipyramid with X in apical position. Only the relevant quartet states and the lowest lying doublet states are shown.

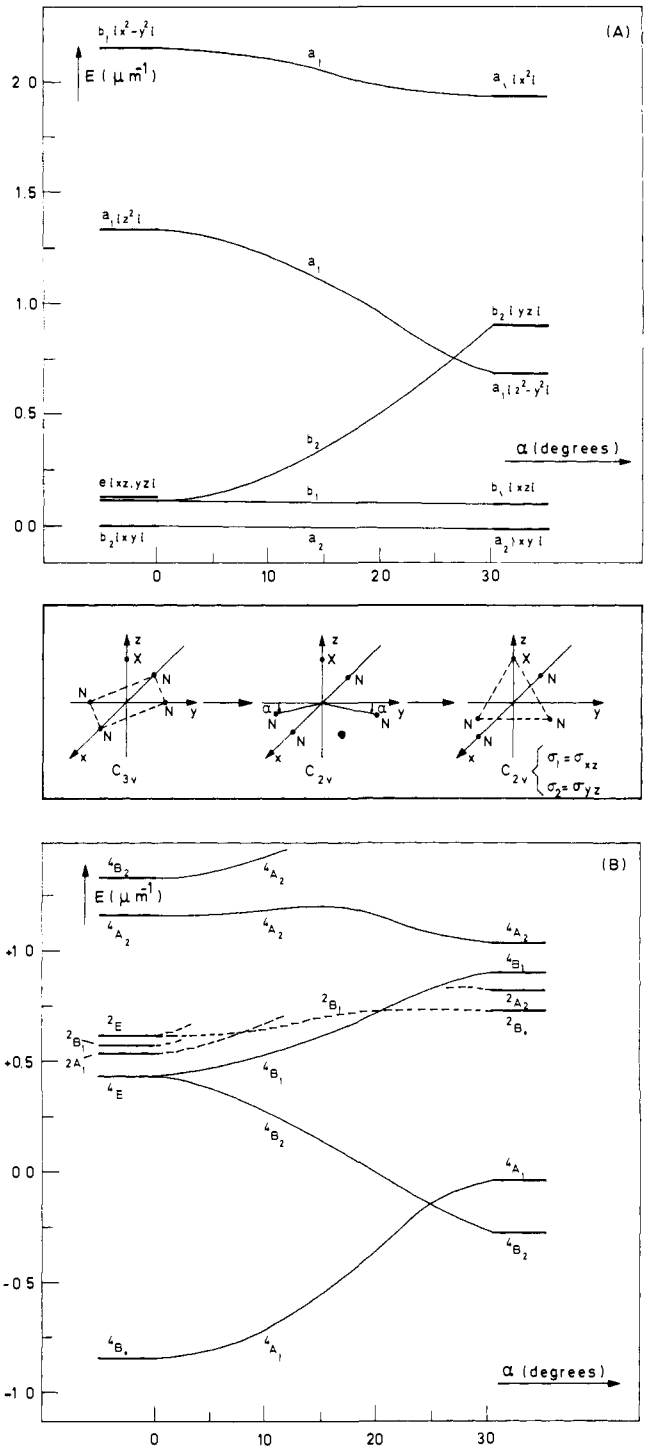

Figure 3. Orbital (A) and state (B) energy correlation diagram for the isomerization of a Cr^{3+} system from the tetragonal pyramid to the trigonal bipyramid with X in equatorial position.

The orbital correlation diagrams for the two conceivable isomerization reactions are shown in Figures 2A and 3A. In Figure 2A the familiar d set (z^2, xz, yz, xy, $x^2 - y^2$) diagonalizes the energy matrix at both sides of the diagram, but not in between; the intermediate symmetry is only C_s. As a consequence of the rearrangement of the ligands, a very strong interaction develops between the a′ orbitals (d_{yz}, d_{z^2}, and $d_{x^2-y^2}$). The highest d orbital starts off as purely $(x^2 - y^2)$; it gains progressively more z^2 character, and ends up as purely z^2. On the other hand, the two a″ orbitals, xz and xy, are virtually unaffected by the variation of the reaction coordinate.

In Figure 3A, the conserved symmetry is C_{2v}; therefore the d_{xy}, d_{xz}, and d_{yz} orbitals remain unaffected along the entire reaction path. The two a_1 orbitals, however, interact with each other and are mixed as α increases. The interaction matrix, given in Table I, applies to the right-hand side of Figure 3A, where the TBP skeleton has been formed. Diagonalization yields

$$d_a = (\sin p)d_{x^2-y^2} - (\cos p)d_{z^2} \quad (1)$$

$$d_b = (\cos p)d_{x^2-y^2} + (\sin p)d_{z^2}$$

Table III. Strong Field Wave Functions[a] of Octahedral Parentage for d^3 Complexes in C_{4v} Symmetry

Irreducible representation in O_h	C_{4v}	Wave function	O_h configuration
$^4A_{2g}$	$^4B_1$	$\|(xz)(yz)(xy)\|$	t_{2g}^3
$^4T_{2g}$	^4E	$\left\|(xz)(xy)\left[\frac{\sqrt{3}}{2}(z^2)-\frac{1}{2}(x^2-y^2)\right]\right\|$	$t_{2g}^2e_g^1$
		$\left\|(yz)(xy)\left[\frac{\sqrt{3}}{2}(z^2)-\frac{1}{2}(x^2-y^2)\right]\right\|$	
	$^4B_2$	$\|(xz)(yz)(x^2-y^2)\|$	
$^4T_{1g}$	^4E	$\left\|(xz)(xy)\left[-\frac{1}{2}(z^2)-\frac{\sqrt{3}}{2}(x^2-y^2)\right]\right\|$	$t_{2g}^2e_g^1$
		$\left\|(yz))xy)\left[-\frac{1}{2}(z^2)-\frac{\sqrt{3}}{2}(x^2-y^2)\right]\right\|$	
	$^4A_2$	$\|(xz)(yz)(z^2)\|$	

[a] Taken from J. R. Perumareddi, *J. Phys. Chem.*, **71**, 3144 (1967).

where

$$tg\ 2p = \frac{2\sqrt{3}(13\sigma_N - 12\pi_N)}{32\sigma_X - 58\sigma_N + 24\pi_N}$$

If X = N, the symmetry is D_{3h}, $tg\ 2p \rightarrow \sqrt{3}$, $p \rightarrow 60°$, and eq 1 becomes

$$d_a = \frac{\sqrt{3}}{2}d_{x^2-y^2} - \frac{1}{2}d_{z^2} = d_{x^2}$$

$$d_b = \frac{1}{2}d_{x^2-y^2} + \frac{\sqrt{3}}{2}d_{z^2} = d_{z^2-y^2} \qquad (2)$$

If the X parameters are not too drastically different from the amine parameters, the composition of d_a and d_b will still be given approximately by eq 2; hence the designations for the two a_1 orbitals on the right-hand side of Figure 3A.

(2) State Correlation Diagrams. Before analyzing the state correlation diagrams, it is useful to take a closer look at the wave functions of the TP starting product, the energies of which are shown in Figure 4. The strong field wave functions (octahedral parentage) for the relevant quartet states are given in Table III.

The tetragonal perturbation is far too weak to modify the multiplicity of the ground state, which remains a quartet characterized by the C_{4v} configuration $e^2b_2^1$. The ^4T states are split, each one giving rise to a ^4E state and another nondegenerate quartet. The lowest ^4E, of $^4T_{2g}$ parentage, is directly correlated with the photoactive ^4E in the hexacoordinated complex; its properties are paramount in the determination of the photosubstitution behavior. The tetragonal perturbation $\mathcal{V}_4$ produces an off-diagonal matrix element between the two ^4E states, which is larger than in the original hexacoordinated complex:

$$(\Psi(^4E;^4T_{2g})|\mathcal{V}_4|\Psi(^4E;^4T_{1g})) = \frac{\sqrt{3}}{2}\left(\sigma_N - \frac{1}{2}\sigma_X\right)$$

The resulting mixing makes the lowest ^4E correspond more closely to a pure $(xz, yz) \rightarrow z^2$ excitation: the z^2 character increases from 75% to 95% or more.

The state correlation diagrams for the Cr(III)-pentacoordinated intermediates are shown in Figures 2B and 3B. At the left-hand side of both figures, the state energies correspond to those of Figure 4.

The degeneracy of the relevant ^4E state is lifted along the reaction path of both Figure 2B and Figure 3B. From a comparison of the two figures, the formation of the TBP with X in equatorial position will obviously be favored with respect to the TBP having X in apical position. The ^4E state under consideration is the prototype of a *stereomobile* state; its $^4B_2$ component will "roll down" spontaneously so as to form the ground state of the appropriate trigonal bipyramid. This can readily be understood from the orbital composition of $^4B_2$ component. Indeed

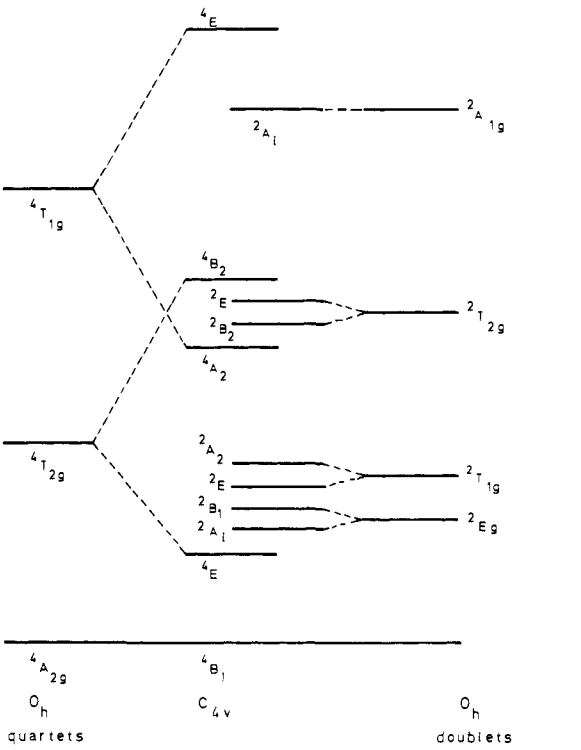

Figure 4. State energy level diagram of a Cr(III) tetragonal pyramid complex; the octahedral parentage is given for the quartets and the doublets separately.

$$\Psi(^4E_a;\ ^4B_2) \simeq |(xz)(xy)(z^2)|$$

$$\Psi(^4E_b;\ ^4B_1) \simeq |(yz)(xy)(z^2)|$$

The d_{z^2} orbital (and to a small extent the $d_{x^2-y^2}$ orbital) are destabilized by the σ^* interaction with the NH_3 ligands in the equatorial plane of the tetragonal pyramid. This antibonding interaction can only be avoided by moving the ligands out of the (xy) plane.

A simultaneous out-of-plane bending of all four equatorial ligands (the a_1 vibrational bending mode) would not constitute an effective relaxation of the ^4E excited state. Indeed, the a_1 bending mode would destabilize *both* d_{xz} and d_{yz}, and since one of these two orbitals is occupied, the ^4E state cannot be expected to undergo a significant stabilization.

Figure 3A, on the other hand, shows the bending of only *two* bonds, situated on the y axis. As a consequence, the energy of the $d_{yz}(b_2)$ orbital increases with increasing values of α. Hereby, the energy of the $^4B_2$ state remains unaffected, since its configuration does not contain the d_{yz} orbital. At the same time the z^2 orbital is gradually transformed into a $d_{z^2-y^2}$ orbital, resulting in a net stabilization of the $^4B_2$ state. At the left-hand side of Figure 3B, the configuration of $^4B_2$ has become approximately $(xz)^1(xy)^1(z^2-y^2)^1$. To the extent that the dissociation of the leaving ligand and the isomerization reaction take place in a concerted way, the stabilization of $^4B_2$ may facilitate the substitution reaction as a whole.

By way of contrast, it is useful to look at the properties of the $^4B_1$ ground state. Neither the reaction path of Figure 2B nor that of Figure 3B offers the possibility to reach a trigonal

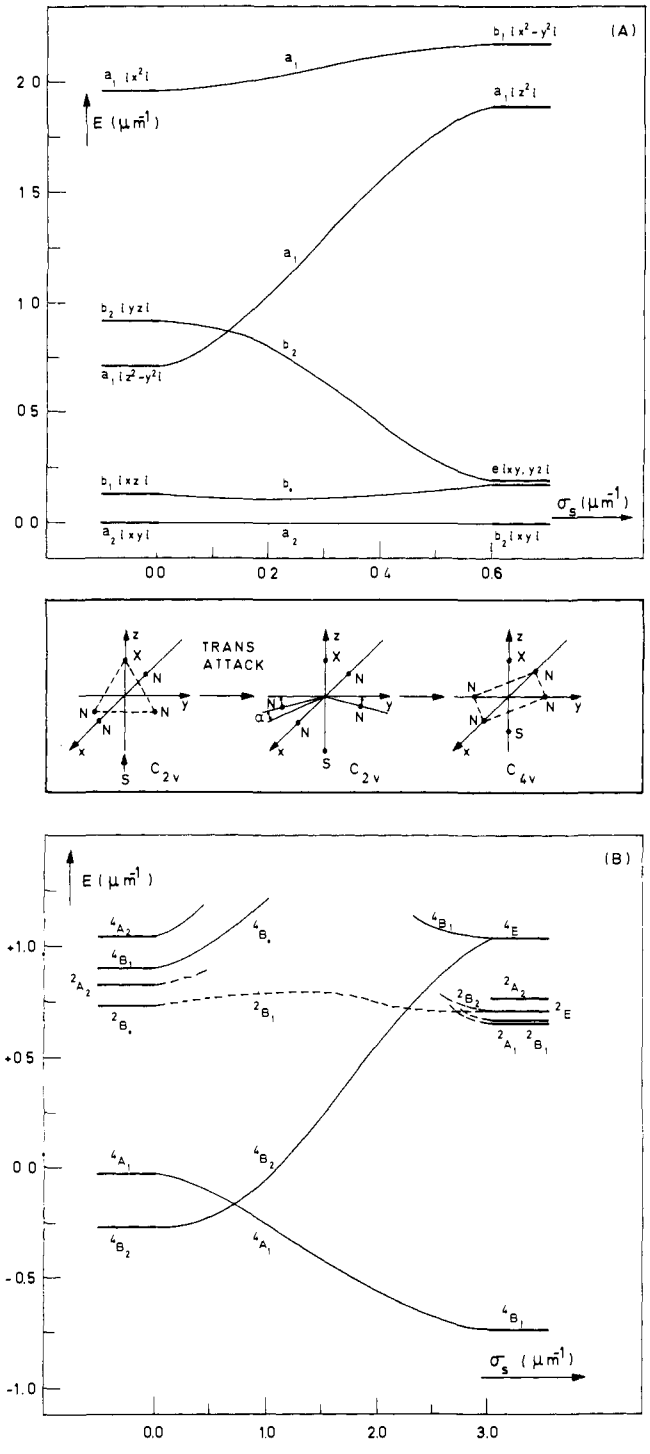

Figure 5. Orbital (A) and state (B) energy correlation diagram for the association reaction by trans attack of a solvent molecule.

bipyramid unless a considerable energy barrier is surmounted. Obviously, the tetragonal pyramid $^4B_1$ state is *stereorigid*. As shown in Table III, its configuration is given by $(xz)^1(yz)^1(xy)^1$.

Since both d_{z^2} and $d_{x^2-y^2}$ are vacant orbitals, there are no σ-antibonding interactions forcing the ligands to move out of place. At the same time, the association of this five-coordinated TP fragment is facilitated: the vacant coordination place has only a very small d-electron density. As stressed already by Hoffmann and Elian,[31] a nucleophilic attack at this point is possible, and gives rise to an octahedral skeleton with trans structure. If the thermal substitution reactions proceed via a dissociative mechanism, their stereoretention could thus readily be understood.

The Association Reaction of the Trigonal Bipyramid. The trigonal bipyramid, with X as an equatorial ligand, acts as a transition state; association with an entering solvent ligand produces another stable hexacoordinated Cr(III) complex. The addition will be assumed to take place in the trigonal plane (edge attack), rather than along another azimuthal angle (face attack). Indeed, from a purely sterical point of view, the central atom is relatively more accessible through the larger (120°) in-plane angles; moreover, edge attack requires the minimum amount of atomic motion to regenerate the octahedron.[32] From the electronic point of view, face attack is also strongly disfavored; this point will be considered when discussing Figure 7.

If the edge association would occur at random, the cis/trans ratio of the product would be 2/1. We will show that the C_{2v} symmetry of the trigonal bipyramid is characterized by a preferential access path, thereby definitely disfavoring the cis attack (with respect to X) over the trans attack. The factors governing the course of the reaction are simply related to the ligand field parameters of X and N.

(1) The Correlation Diagrams. Figures 5 and 6 show the orbital and the state energy correlation diagrams for a trans and a cis attack of a solvent molecule S with respect to the heteroligand X. The association reaction has been analyzed as a decrease of the Cr–S distance, combined with a concerted decrease of two ligand–metal–ligand angles (Ψ) from 120° to 90°. Within the framework of the present ligand field model, the change in Cr–S distance has been accounted for by increasing σ_S from zero to its equilibrium value σ_S^0; at all points σ_S/π_S was kept constant. The concertation between radial and angular movements can be realized by using an expression of the type

$$\sigma_S = \sigma_S^0\left(\frac{\alpha}{30}\right) \text{ or } \sigma_S = \sigma_S^0\left(\frac{\alpha}{30}\right)^{1/2}$$

where $\alpha = 120° - \Psi$. Both possibilities lead to very similar results. The curves shown in Figures 5 and 6 correspond to the second (square root) alternative, simulating an association reaction, where the entering ligand is the dominant factor at the outset of the process.

The zero-order strong field wave functions of the two lowest TBP quartet states are given by

$$\Psi(^4B_2) = |(xy)(xz)(z^2 - y^2)| \qquad (a_2^1b_1^1a_1^1)$$

$$\Psi(^4A_1) = |(xy)(xz)(yz)| \qquad (a_2^1b_1^1b_2^1)$$

for the ground and the first excited state, respectively. It was pointed out already that the a_1 orbital in $^4B_2$ is not purely $z^2 - y^2$. The numerical calculation with the parameter set of Table II yields for p in eq 1 a value of 63° instead of 60°, a very small effect indeed. The introduction of electron repulsion and configuration interaction within the ligand field state manifold shows that the two states under consideration are characterized in a rather pure way by the indicated single configurations. This allows us to visualise the general features of the electron density in a very simple way. Both in $^4B_2$ and in $^4A_1$ the d_{xz} and d_{xy} orbitals are occupied; this gives rise to an axial-symmetric electron density distribution along the x direction on both sides of the yz plane. This effectively narrows down the access possibilities to an equatorial approach of the incoming ligand. Figure 7 shows the relevant orbitals in this plane. The $^4B_2$ state is characterized by a vacant d_{yz} orbital; it is obvious from the figure that this orbital has directional properties, which are very favorable for a cis attack. The σ antibonding induced by the new metal–ligand interaction will be carried by the vacant orbital. This is the more so, as the neighboring ligands X and N have at their disposition an energetically favorable path to complete the equatorial square. In the final hexacoordinated complex, the occupied $(z^2 - y^2)$ orbital becomes a normal π

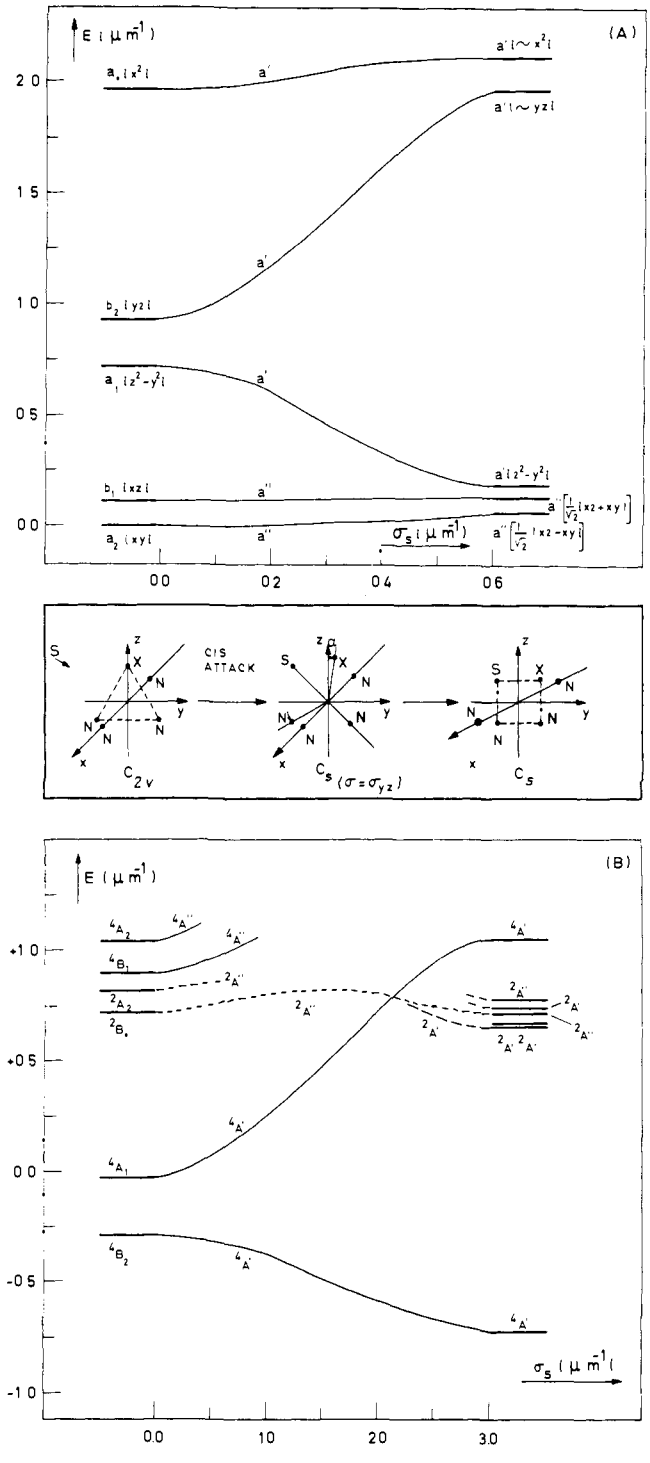

Figure 6. Orbital (A) and state (B) energy correlation diagram for the association reaction by cis attack of a solvent molecule.

antibonding orbital, while the empty (yz) orbital is a σ antibonding metal orbital.

The trans attack, on the other hand, is hindered by precisely the same factors that facilitate the cis attack: the motions of both the incoming ligand and of the two N-neighboring ligands will be such that the occupied ($z^2 - y^2$) orbital will be greatly destabilized, whereas the empty (yz) orbital becomes stabilized.

Therefore, a cis attack on the $^2B_2$ ground state of the TBP is correlated to the ground state of the hexacoordinated complex with no energy barrier in between, while a trans attack on the same state correlates with an excited state of the reaction product.

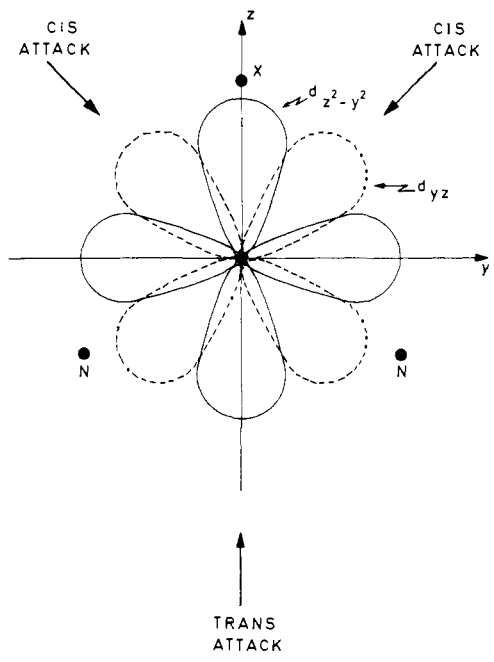

Figure 7. The d orbitals in the equatorial yz plane of the trigonal bipyramid.

The $^4A_1$ state is characterized by exactly the opposite situation, since the electron is now transferred from ($z^2 - y^2$) to yz.

(2) Connection with Axial Labilization.[6] Basically, the stereospecific reaction mode of the trigonal bipyramid can be traced back to the symmetry lowering of the ligand field Hamiltonian. The equatorial introduction of the heteroligand X reduces the symmetry from D_{3h} to C_{2v}; as a consequence, the degenerate orbital set ($yz, z^2 - y^2$) gives rise to two different energies.

The relative energy and the electron occupancy of these two orbitals govern the equatorial access possibilities. The occupancy of d_{yz} is trans orienting; the occupancy of $d_{z^2-y^2}$ is cis orienting. In the preceding section, we stressed that these two orbitals are found back nearly unchanged in the $^4A_1$ and $^4B_2$ states, respectively. To first order, both states are also characterized by the same electron repulsion energy: they can be seen as derived from the same parent D_{3h} $^4E'$ state. Therefore

$$E(^4A_1) - E(^4B_2) \simeq E(d_{yz}) - E(z^2 - y^2) = \frac{1}{4}(10Dq_N - 10Dq_X)$$

This equation suggests an obvious connection with the factors responsible for the determination of the leaving ligand.[6] According to Adamson's first rule, the photoexcitation labilizes the axis characterized by the weakest ligand field. The here considered *trans*-CrN_4XY complexes all satisfy this rule: the leaving ligand is situated on the heteroaxis, and

$$\overline{Dq}_{ax} = \frac{Dq_X + Dq_Y}{2} < \overline{Dq}_{eq} = Dq_N$$

More specifically, in all cases known so far, $Dq_X < Dq_N$. Therefore, the actual situation is realistically described by Figures 5 and 6 and only cis formation is observed.

(3) The Fluoride Case. The composition of the $d_{z^2-y^2}$ orbitals is 75% d_{z^2} for a perfect D_{3h} symmetry ($p = 60°$). For a typical π-donor X ligand, p is calculated to be 63°: the d_{z^2} character increases to approximately 79%. The deviation from the zero-order situation can be seen most easily by transforming the two by two a_1 interaction matrix of Table I to a more ap-

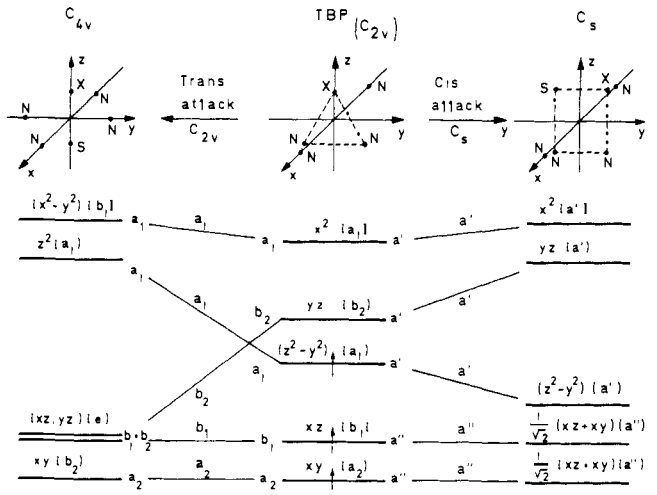

Figure 8. Comparative qualitative orbital energy correlation diagrams of Woodward-Hoffmann type for cis and trans attack in the association reaction.

propriate basis suggested by eq 2:

$\mathcal{V}$	x^2	z^2-y^2
x^2	$\frac{1}{4}\sigma_X+\frac{5}{2}\sigma_X$	$\frac{\sqrt{3}}{4}(\sigma_N-\sigma_X)$
z^2-y^2	$\frac{\sqrt{3}}{4}(\sigma_N-\sigma_X)$	$\frac{3}{4}\sigma_X+\frac{3}{8}\sigma_N+\frac{3}{2}\pi_N$

If $\sigma_N > \sigma_X$, the usual case for an average π donor, the z^2 percentage of the lowest a_1 orbital increases. This reinforces even more the preference of a cis attack over trans attack, since entry of the S ligand along the z axis is made more difficult. If, however, $\sigma_N < \sigma_X$, as is the case of F^-, the z^2 character of the lowest a_1 orbital drops below 75%; this tends to render the trans attack less hindered. It is remarkable that the only case with a significant trans production (up to 9% of the total quantum yield)[15] is precisely *trans*-$Cr(en)_2FCl^+$, where the resulting trigonal bipyramid is $Cr(en)_2F^{2+}$.

Discussion and Conclusions

(1) It has been shown that the factors determining the photochemistry of Cr(III) complexes are basically the same factors that also determine the selective photolabilization of one particular ligand. The same ligand field parameters that are responsible for the energetic evolution of a particular set of orbitals and states are also decisive in the evaluation of the relative bond strengths (I*) in the photoactive state.[6]

The purely dissociative reaction mechanism that was formally adopted in our earlier leaving ligand treatment has been complemented in the present paper by the study of the two remaining reaction steps. The photosubstitution can thus be regarded as a succession of three more or less concerted processes, all governed by a given set of ligand field parameters.

(2) In the isomerization reactions, the evolution of the orbital energies along a given path appears to follow a very simple rule. The ligands move in such a way that they avoid the occupied orbitals, and that they are directed toward spatial zones, where vacant orbitals have large probability densities. Therefore the ligand movement, characteristic of an actual reaction path, tends to increase the energy of the vacant d orbitals and to decrease the energy of the occupied orbitals.

Similar considerations have been successfully applied in predicting and rationalizing the *shapes* of transition metal complexes.[33] This is not to imply that a simple rule of this type would be of general validity in transition metal chemistry as a whole. It is certainly to be expected that in some cases configuration interaction, or even spin-orbit coupling, might become sufficiently important, so as to modify a presumed reaction path significantly.

(3) The association reactions and the corresponding correlation diagrams might be interpreted in terms of Fukui's frontier orbitals.[34] A ligand approaching a molecular fragment will preferably do so along an access path containing vacant d orbitals. The donor levels of the ligand act as HOMOs, while the d orbitals act as LUMOs.

(4) An alternative way of analyzing the association reactions is by using the Woodward-Hoffmann methodology. In the middle of Figure 8 the orbital energies of the trigonal bipyramid are shown. For the reaction path corresponding to cis attack (right-hand side) the conserved symmetry is C_s; both the orbitals of the reagent and the product are labeled as irreducible representiations of this point group. The principle of conservation of orbital symmetry allows one to draw the correlation lines without any ambiguity. The same procedure is repeated for the trans attack on the left-hand side; here the conserved symmetry is C_{2v}. It is quite obvious that the comparison of the two reaction modes gives rise to a clear-cut selection rule: the cis attack is an allowed process, the trans attack is a forbidden process. This conclusion is independent of the specific values of the orbital energies and of the ligand field parameters—at least all the cases reported in the literature can be accommodated into this scheme.

It may be well to stress here that the orbital occupation is of course quite different here from what one is used to in typical organic reactions, as in the original Woodward-Hoffmann considerations. This remark points to the very important role played by electron repulsion in the open shell d^n systems. Actually, in coordination chemistry even more than in organic chemistry, one should draw conclusions only from state correlation diagrams. For the association reaction under consideration, such a diagram can quite easily be constructed either from Figure 8 or from Figures 5B and 6B. It appears that, at least in the present case, the conclusions from orbital and state correlation diagrams are in complete agreement. In general, however, the only safe way to proceed is via state energy correlation diagrams.

Provided that due attention is given to this latter point, it may be hoped that the introduction of electronic selection rules on the basis of symmetry conservation will offer a fruitful approach to the field of coordination chemistry.

References and Notes

(1) V. Balzani and V. Carassiti, "Photochemistry of Coordination Compounds", Academic Press, New York, N.Y., 1970.
(2) E. Zinato in "Concepts of Inorganic Photochemistry", A. W. Adamson and P. D. Fleischauer, Ed., Wiley-Interscience, New York, N.Y., 1975.
(3) A. W. Adamson, *J. Phys. Chem.*, **71**, 798 (1967).
(4) J. I. Zink, *J. Am. Chem. Soc.*, **96**, 4464 (1974).
(5) M. Wrighton, H. B. Gray, and G. S. Hammond, *Mol. Photochem.*, **5**, 164 (1973).
(6) L. G. Vanquickenborne and A. Ceulemans, *J. Am. Chem. Soc.*, **99**, 2208 (1977).
(7) A. D. Kirk, *Mol. Photochem.*, **5**, 127 (1973).
(8) A. D. Kirk, K. C. Moss, and J. G. Valentin, *Can. J. Chem.*, **49**, 1524 (1971).
(9) C. Bifano and R. G. Linck, *Inorg. Chem.*, **13**, 609 (1974).
(10) M. T. Gandolfi, M. F. Manfrin, A. Juris, L. Moggi, and V. Balzani, *Inorg. Chem.*, **13**, 1342 (1974).
(11) P. Riccieri and E. Zinato, Proceedings of the XIV International Conference on Coordination Chemistry, Toronto, Canada, June 1972.
(12) E. Zinato, P. Riccieri, and A. W. Adamson, *J. Am. Chem. Soc.*, **96**, 375 (1974).
(13) C. F. C. Wong and A. D. Kirk, *Inorg. Chem.*, **15**, 1519 (1976).
(14) M. F. Manfrin, L. Moggi, and V. Balzani, *Inorg. Chem.*, **10**, 207 (1971); A. D. Kirk, *J. Am. Chem. Soc.*, **93**, 283 (1971).
(15) G. Wirth and R. G. Linck, *J. Am. Chem. Soc.*, **95**, 5913 (1973).
(16) C. Kutal and A. W. Adamson, *J. Am. Chem. Soc.*, **93**, 5581 (1971).
(17) Cyclam stands for 1,4,8,11-tetraazacyclotetradecane.
(18) C. Kutal and A. W. Adamson, *Inorg. Chem.*, **12**, 1990 (1973).
(19) H. Yamatera, *Bull. Chem. Soc. Jpn.*, **31**, 95 (1958); D. S. McClure in "Advances in the Chemistry of Coordination Compounds", S. Kirschner, Ed., Macmillan, New York, N.Y., 1961, p 498.

(20) C. E. Schäffer, "XIIth International Conference on Coordination Chemistry, Sydney 1969", IUPAC, Butterworths, London, 1970, p 316.
(21) C. K. Jørgensen, "Modern Aspects of Ligand Field Theory", Elsevier, Amsterdam, 1971, Chapter 13.
(22) L. G. Vanquickenborne, J. Vranckx, and C. Görller-Walrand, *J. Am. Chem. Soc.*, **96**, 4121 (1974); J. Vranckx and L. G. Vanquickenborne, *Inorg. Chim. Acta*, **11**, 159 (1974); C. Görller-Walrand and L. G. Vanquickenborne, *J. Mol. Struct.*, **19**, 737 (1973).
(23) J. S. Griffith, "The Theory of Transition-Metal Ions", Cambridge University Press, New York, N.Y., 1964.
(24) Y. Tanabe and S. Sugano, *J. Phys. Soc. Jpn.*, **9**, 753 (1951).
(25) R. B. Woodward and R. Hoffmann, *Angew. Chem., Int. Ed. Engl.*, **8**, 781 (1969).
(26) H. C. Longuet-Higgins and E. W. Abrahamson, *J. Am. Chem. Soc.*, **87**, 2045 (1965).
(27) T. H. Whitesides, *J. Am. Chem. Soc.*, **91**, 2395 (1969); see also D. R. Eaton, *ibid.*, **90**, 4272 (1968).
(28) A. R. Rossi and R. Hoffmann, *Inorg. Chem.*, **14**, 365 (1975).
(29) J. Glerup, O. Mønsted, and C. E. Schäffer, *Inorg. Chem.*, **15**, 1399 (1976).
(30) W. W. Fee and J. N. MacB. Harrowfield, *Aust. J. Chem.*, **23**, 1049 (1970).
(31) M. Elian and R. Hoffmann, *Inorg. Chem.*, **14**, 1058 (1975).
(32) F. Basolo and R. G. Pearson, "Mechanisms of Inorganic Reactions", Wiley, New York, N.Y., 1967, Chapter 4; M. L. Tobe, "Inorganic Reaction Mechanisms", Studies in Modern Chemistry, Nelson, London, 1972, Chapter 7.
(33) J. K. Burdett, *Inorg. Chem.*, **14**, 375 (1975).
(34) The frontier electron concept was pioneered by Fukui: K. Fukui, *Top. Curr. Chem.*, **15** (1970).

Charge-Transfer Interactions between Transition Metal Hexafluorides and Xenon†

J. D. Webb and E. R. Bernstein*

Contribution from the Department of Chemistry, Colorado State University, Fort Collins, Colorado 80523. *Received July 5, 1977*

Abstract: Charge transfer transitions are reported for MF_6 (M = W, Mo, U, Re, Ir) with Xe. The nature of the charge transfer complexes is discussed. Based on spectroscopic data new estimates of MF_6 electron affinities are presented.

I. Introduction

In the course of spectroscopic studies of paramagnetic transition metal hexafluorides, it became apparent that additional information might be obtained if a high-symmetry host material for mixed crystals could be found. Such systems would be particularly useful for the study of the Γ_{8g} (O_h*) states, in which the Jahn–Teller interaction is of particular interest.[1,2] It was thought that xenon might serve as a good host; it has no crystal vibrational frequencies in the range of intramolecular MF_6 vibrations, and size and orientation considerations indicate that MF_6 might go into the Xe lattice substitutionally. However, it was found that when IrF_6, which is yellow, is dissolved in liquid Xe, the solution is totally opaque, although purple in reflection. It is the purpose of this paper to demonstrate that the new absorption band for the IrF_6–Xe system is due to a low-lying intermolecular charge transfer (CT) transition between Xe and MF_6:

$$Xe + MF_6 \xrightarrow{h\nu} Xe^+MF_6^-$$

Such CT transitions and associated complexes with MF_6 are known,[3] but have not been previously observed for the rare gases.

Several experiments have been carried out to verify these conclusions and to increase understanding of this phenomenon. The absorption spectra of MF_6–Xe (M = Ir, Re, W, Mo, U) at liquid nitrogen temperature have been taken. An IrF_6–Kr sample and a gas-phase IrF_6–Xe sample were also prepared and investigated. Besides demonstrating the CT nature of the new transitions, these experiments also give valuable information on the exceptionally high electron affinities of the hexafluorides. Observation of "local" (intramolecular) IrF_6 transitions in the near IR also permits conclusions to be drawn concerning stability of the IrF_6–Xe complex.

† Supported in part by the Office of Naval Research.

II. Experimental Section

Handling of hexafluorides has been previously described.[1] Research grade xenon and krypton (Linde) were used and were further purified by distillation to remove any traces of H_2O, a very serious impurity for the hexafluorides.

Crystals were grown from the melt by suspending the sample cell a few centimeters above the surface of liquid nitrogen in a closed Dewar. Although crystals grown this rapidly (~20 min) are certainly not high-quality single crystals, they are of adequate quality to allow spectra to be taken. Visible and near-UV absorption spectra were taken on a McPherson 285 monochromator with photoelectric detection. Near-IR spectra were obtained on a McPherson 2051 with a 77K InAs (Texas Instruments) detector. Some preliminary spectra were also obtained on a Cary 17.

III. Theory

The theory of CT transitions and complexes is well known[4] and will be outlined only briefly here. For 1:n complexes (in this case n is either 12Xe or 1Xe), the energy of the CT transition is

$$h\nu_{CT} = I_d - E_a + (G_1 - n'G_0) + (X_1 - n'X_0) \quad (1)$$

in which I_d = ionization potential of the donor D (Xe), E_a = electron affinity of the acceptor A (MF_6), G_1 = "normal" interaction of D^+ and A^-, specifically neglecting the CT interactions, G_0 = "normal" interaction of D and A, X_1 = additional interaction between D^+ and A^- due to proximity of D–A configuration, X_0 = additional interaction between D and A due to proximity of the D^+–A^- configuration, n = number of donors in the complex, and in the limit of weak complexes, n' = n. For stronger complexes $n' < n$ due to saturation effects.[5]

X_0 can be approximated by second-order perturbation theory as

$$X_0 \sim -\frac{\beta_0^2}{\Delta} \quad (2)$$

0002-7863/78/1500-0483$01.00/0